The enhancement of coseismic slip and ground motion due to the accretionary wedge and sedimentary layer in the 2011 Tohoku-Oki earthquake

Xian Li[1,1] and Yihe Huang[2,2]

[1]Institute of Geology and Geophysics
[2]University of Michigan-Ann Arbor

November 30, 2022

Abstract

Low-velocity accretionary wedges and sedimentary layers overlying continental plates widely exist in subduction zones. However, the two structures are commonly neglected in velocity models used in slip inversion, ground motion estimation, and dynamic rupture simulation, which may cause a biased estimation of coseismic slip and near-fault ground motions during subduction zone earthquakes. We use the 2011 Mw 9.0 Tohoku-Oki earthquake as an example and reproduce the observed seafloor deformation using 2-D dynamic rupture models with or without an accretionary wedge and a sedimentary layer. We find that the co-existence of the accretionary wedge and sedimentary layer significantly enhances the shallow coseismic slip and amplifies ground accelerations near the accretionary wedge. Hence, stress drop on the shallow fault estimated from the coseismic slip or surface deformation is overestimated when the two structures are neglected. We further simulate a suite of earthquakes where the up-dip rupture terminates at different depths. Results show that a sedimentary layer enhances coseismic slip in all cases, while an accretionary wedge can lead to a sharper decline in slip when negative dynamic stress drop exists on the shallow fault. However, a combination of the two structures tends to enhance fault slip, especially when rupture breaks through a trench. Thus, their combined effects are nonlinear and can be larger than the respective contribution of each structure. Our results emphasize that subduction zones featuring a co-existence of an accretionary wedge and a sedimentary layer may have inherently higher earthquake and tsunami hazards.

Hosted file

essoar.10506336.2.docx available at https://authorea.com/users/561642/articles/608996-the-enhancement-of-coseismic-slip-and-ground-motion-due-to-the-accretionary-wedge-and-sedimentary-layer-in-the-2011-tohoku-oki-earthquake

The relative effects of the accretionary wedge and sedimentary layer on the rupture process of subduction zone earthquakes

Xian Li[1 2], Yihe Huang[3]

[1]Key Laboratory of Earth and Planetary Physics, Institute of Geology and Geophysics, Chinese Academy of Sciences, Beijing 100029, China.

[2]College of Earth and Planetary Sciences, University of Chinese Academy of Sciences, Beijing 100049, China.

[3]Department of Earth and Environmental Sciences, University of Michigan, Ann Arbor, MI 48109, USA.

Corresponding author: Xian Li (lixian@mail.iggcas.ac.cn)

Key Points:

- Our rupture simulations unveil the relative effects of accretionary wedges and sedimentary layers on earthquake slip and ground motions.
- The two structures can have opposite effects on slip, but their co-existence always enhances fault slip and amplifies ground motions.
- The enhancement effect on fault slip increases with shallower up-dip rupture extent and hence earthquake magnitude.

Abstract

Low-velocity accretionary wedges and sedimentary layers overlying continental plates widely exist in subduction zones. However, the two structures are commonly neglected in velocity models used in slip inversion, ground motion estimation, and dynamic rupture simulation, which may cause a biased estimation of coseismic slip and near-fault ground motions during subduction zone earthquakes. We use the 2011 M_w 9.0 Tohoku-Oki earthquake as an example and reproduce the observed seafloor deformation using 2-D dynamic rupture models with or without an accretionary wedge and a sedimentary layer. We find that the co-existence of the accretionary wedge and sedimentary layer significantly enhances the shallow coseismic slip and amplifies ground accelerations near the accretionary wedge. Hence, stress drop on the shallow fault estimated from the coseismic slip or surface deformation is overestimated when the two structures are neglected. We further simulate a suite of earthquakes where the up-dip rupture terminates at different depths. Results show that a sedimentary layer enhances coseismic slip in all cases, while an accretionary wedge can lead to a sharper decline in slip when negative dynamic stress drop exists on the shallow fault. However, a combination of the two structures tends to enhance fault slip, especially when rupture breaks through a trench. Thus, their combined effects are nonlinear and can be larger than the respective contribution of each structure. Our results emphasize that subduction zones featuring a co-existence of an accretionary wedge and a sedimentary layer may have inherently higher earthquake and tsunami hazards.

Plain Language Summary

The accretionary wedge and sedimentary layer are two low-velocity sediment structures widely existing in subduction zones, which can have a great impact on earthquake processes and ground motions. In the 2011 M_w 9.0 Tohoku-Oki earthquake, rupture propagated to the trench with large fault slip on the shallow fault. Our earthquake simulations reveal that considering both structures in the northern Japan trench significantly enhances shallow fault slip during the 2011 M_w 9.0 Tohoku-Oki earthquake. By simulating a suite of earthquake scenarios with different rupture extents, we find that the enhancement effects of an accretionary wedge and a sedimentary layer

on fault slip are especially pronounced when rupture reaches the trench and yet diminish as the up-dip rupture extent becomes deeper. These structures also significantly amplify and prolong ground motions for both large and small earthquakes. Subduction zones that feature a co-existence of the two structures may have a greater potential to accommodate large earthquakes due to their enhancement effects on fault slip.

1. Introduction

Sediments play a key role in the mechanical processes of subduction zones. In the collision margin where an oceanic plate subducts below a continental plate, material offscraped from the downgoing oceanic plate forms a wedge-shaped low-velocity sediment zone called an accretionary wedge. Accretionary wedges are widely observed in subduction zones (Table 1). For example, in the northern Japan trench where the 2011 Tohoku-Oki earthquake occurred, a wedge-shaped sedimentary unit with P-wave velocities of 2.0-4.0 km/s is located at the seaward end of the continental plate and extends to a depth greater than 13 km (Tsuru et al., 2002). The accretionary wedge in the eastern Nankai trough consists of five layers having seismic velocities of 1.8, 1.9-2.7, 2.8-3.5, 3.8-4.6, and 4.6-5.3 km/s (Nakanishi et al., 1998). In the Cascadia subduction zone, the accretionary wedge is wide from Vancouver to northern Oregon but is narrow from southern Oregon to northern California (Gulick et al., 1998). Along the Peru-Chile trench, the size of the frontal accretionary complex is variable, with accreted sediments appearing in the margin of south-central Chile but absenting in Peru (Flueh et al., 1998; Krabbenhöft et al., 2004).

Besides accretionary wedges, sedimentary layers overlying continental plates are common features in subduction zones, as shown by the map of *Total Sediment Thickness of the World's Oceans and Marginal Seas* (Divins, 2003). In Sumatra, north Japan, Aleutians, Cascadia, and central Chile, nearshore deposits accumulated on the continental margins, making up the several kilometers thick sedimentary layers. These sedimentary layers have relatively lower P-wave velocities of 2-3 km/s compared to accretionary wedges, which complicates the lateral material variation (Table 1). Taking the northern Japan trench, eastern Nankai trough, and middle Ryukyu trench as examples, the conceptual diagrams in Figure 1 demonstrate three simplified scenarios about the distribution of sediments on the overriding plate. In the northern Japan trench, both the accretionary wedge and sedimentary layer are observed. The eastern Nankai trough has an accretionary wedge but no sedimentary layer, whereas there are only sedimentary layers in the middle Ryukyu trench.

Table 1. Dimensions and P-wave velocities of accretionary wedges and sedimentary layers in subduction zones

Subduction Zone	Accretionary wedge		Sedimentary layer		Reference
	Width (km)	P-wave velocity (km/s)	Thickness (km)	P-wave velocity (km/s)	
Makran	>100	1.8-4.4	N/A	N/A	Kopp et al., 2000
Sumatra	30	3.0-3.9	3-5	2.0-3.0	Kopp et al., 2001
Ryukyu trench	N/A	N/A	9	1.8-4.7	Kodaira et al., 1996
Nankai trough	150	1.8-5.3	N/A	N/A	Nakanishi et al., 1998
North Japan trench	40-60	2.0-4.0	2	1.7-2.4	Tsuru et al., 2002; Kimura et al., 2012
South Kuril	10	2.4-3.7	1-2	1.9-2.1	Klaeschen et al., 1994
Central Kuril	N/A	N/A	1-2	1.9-2.2	Klaeschen et al., 1994
North Kuril	18	2.4-2.8	1-2	2.0-2.2	Klaeschen et al., 1994
Aleutians	20-30	2.5-4.5	2-3	2.0-3.0	Holbrook et al., 1999
Alaska	30	1.5-4.5	1-2	1.5-2.4	Brocher et al., 1994; von Huene et al., 1998
Cascadia	50-100	4.5-5.0	3-5	2.0-3.0	Gulick et al., 1998; Parsons et al., 1998
Costa Rica	N/A	N/A	2-4	2.2-4.0	Sallarès et al., 2001
Peru	N/A	N/A	1-3	1.7-3.0	Krabbenhöft et al., 2004
Central Chile	35-50	3.0-4.0	1-3	2.0-2.3	Flueh et al., 1998

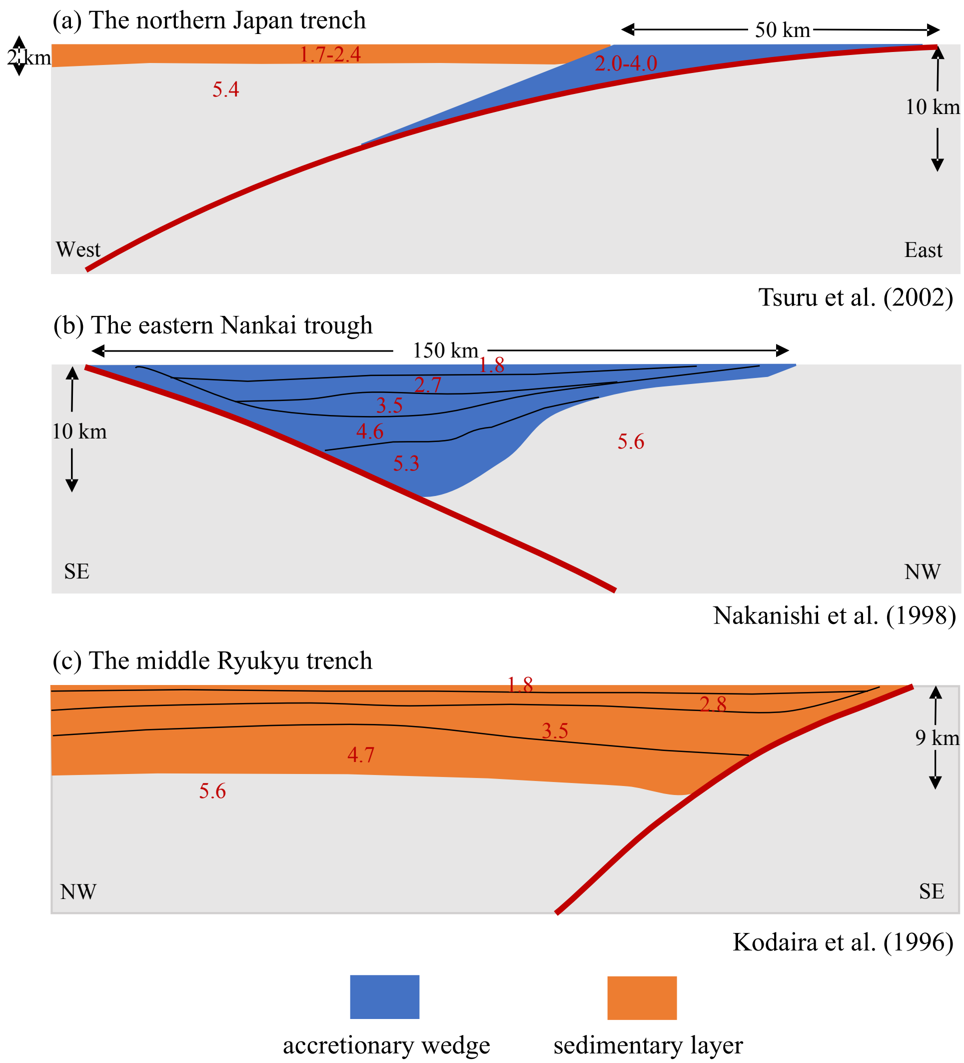

Figure 1. Conceptual diagrams showing sediment distribution on the overriding plate. (a) Co-existence of an accretionary wedge and a sedimentary layer. (b) Existence of an accretionary wedge only. (c) Existence of sedimentary layers only. Bold red curves represent the plate interface. The accretionary wedge is shown in blue, and the sedimentary layer is shown in orange. The numbers denote P-wave velocities (km/s) (Tsuru et al., 2002; Nakanishi et al., 1998; Kodaira et al., 1996).

In the last century, M_w 8.5 and above earthquakes occurred in the Sumatra, north Japan, Kuril, Kamchatka, Aleutians, Alaska, and south-central Chile subduction zones. These subduction zones all feature a co-existence of accretionary wedges and sedimentary layers, which can have a great impact on coseismic slip and ground motions of subduction zone earthquakes in two aspects: 1) The low-velocity materials cause larger strain given the same stress according to Hooke's Law, which means larger coseismic slip at the base of accretionary wedges and larger deformation on the surface of sediments; 2) Reflected waves generated within these low-velocity structures can modulate rupture dynamics and induce high-frequency ground motions. Numerical models conducted by Lotto et al. (2017) and Zelst et al. (2019) suggested that more compliant accretionary wedges in subduction zones cause greater shallow slip. Ma and Hirakawa (2013) demonstrated that the Coulomb failure in the overriding wedge tends to give rise to significant seafloor uplift and depletion in the high-frequency radiation in dynamic rupture simulations. Kozdon and Dunhuam (2013) and Murphy et al. (2018) explored dynamic rupture models with depth-dependent material properties to understand rupture processes of megathrust earthquakes. However, these models neglected the top sedimentary layer that has even lower P-wave velocities than accretionary wedges. Although such a layer is thin in some subduction zones (Table 1), it can have a significant impact on rupture processes. Moreover, in subduction zones having both an accretionary wedge and a sedimentary layer, the combined effects of the two structures on earthquake rupture processes and ground motions are yet unclear.

Here we first use the M_w 9.0 Tohoku-Oki earthquake rupture as an example to understand the role of accretionary wedges and sedimentary layers. We choose this earthquake as its source process is constrained by abundant observations, including seafloor geodetic observations (Kido et al.,2011; Sato et al., 2011), ocean-bottom pressure gauge data (Ito et al., 2011), and multibeam bathymetric data (Fujiwara et al., 2011). Slip inversions based on seismic recordings, geodetic data, tsunami data, and combinations of different data sets supported huge coseismic slip (> 50 m) in the shallow region of the plate boundary (Lay, 2018). A number of dynamic rupture models have been proposed for the 2011 Tohoku-Oki earthquake to elucidate the rupture process, and they mainly focused on the effects of fault friction and stress state on slip distribution and rupture propagation (Kato and Yoshida, 2011; Duan, 2012; Mitsui et al., 2012; Huang et al., 2012 and 2014; Noda and Lapusta, 2013; Kozdon and Dunham, 2013; Cubas et al., 2015). However, most slip inversion models and dynamic rupture simulations were based on an elastic homogeneous medium or a 1-D layer model neglecting the low-velocity accretionary wedge and sedimentary layer, which may cause a biased estimation of coseismic slip, stress drop, and ground motions. With both the accretionary wedge and sedimentary layer widely overlying the continental plate in the northern Japan trench (Tsuru et al., 2002), it is instrumental to understand the separate and combined effects of these near-source structures on the large seafloor deformation near the trench during the 2011 Tohoku-Oki earthquake.

As most seafloor deformation observation in the 2011 Tohoku-Oki earthquake concentrated in a direction perpendicular to the trench, we use a 2-D dynamic model to reproduce the observed deformation of the 2011 Tohoku-Oki earthquake by considering an accretionary wedge (aw) and a thin sedimentary layer (sed) overlying the continental plate (aw-and-sed model) (Figure 1a). Compared to a homogeneous medium, our results show that the co-existence of the accretionary wedge and sedimentary layer greatly enhances the coseismic slip on the shallow fault and amplifies ground accelerations near the accretionary wedge. We also show that stress drop on the shallow fault estimated from the coseismic slip or surface deformation is overestimated when the two structures are neglected. We further explore the effects of an accretionary wedge and a sedimentary layer by simulating a range of earthquakes with different rupture extents. We find that a sedimentary layer always enhances coseismic slip in different earthquake scenarios. While an accretionary wedge may reduce near-trench slip when the shallow fault features negative dynamic stress drop, a combination with sedimentary layers tends to enhance shallow slip instead. The enhancement effects on coseismic slip are especially pronounced when rupture breaks through the trench. As the up-dip rupture is deeper, the two structures have a smaller impact on fault slip but still greatly amplify ground accelerations on the overriding plate. We also discuss how our dynamic rupture models can be applied as reference scenarios to earthquake hazard analysis in global subduction zones where accretionary wedges or sedimentary layers exist.

2. Model setup

We use a 2-D dynamic rupture model containing the main features of the northern Japan trench to reproduce the observed seafloor deformation of the 2011 Tohoku-Oki earthquake. In order to model the earthquake rupture process as realistically as possible, we apply observation data including seismic profile, geology survey, drilling site to constrain our model parameters (Tsuru et al., 2002; Kimura et al., 2012; Ujiie et al., 2013). To isolate the contributions of the accretionary wedge and sedimentary layer on coseismic slip and ground accelerations, we compare the aw-and-sed model to three models that only contain an accretionary wedge (aw-only model), a sedimentary layer (sed-only model), and a homogeneous medium (homogeneous model) with the same friction and stress parameters as the aw-and-sed model. An accretionary wedge is located within 50 km landward from the Japan trench axis on the surface and extends to 10 km in depth. A 2-km-thick sedimentary layer overlies the continental plate outside the accretionary wedge (Figure 1a). We use P-wave velocities of 2.0 km/s, 4.0 km/s, 5.4 km/s in the accretionary wedge, sedimentary layer, and surrounding zone respectively, in accordance with the seismic survey in the northern Japan trench (Tsuru et al., 2002). We set the Poisson's ratio to 0.25 and the density to 3000 kg/m^3 throughout the whole domain. The top of the model domain is a free surface, and an absorbing boundary is applied to the out-most margin to avoid artificial reflections. A 200-km-wide fault with dip angles gradually changing from 6° at the surface to 16° at a depth of 50 km is embedded in an elastic half-space. The hypocenter is located at a depth of 21 km (Chu et al., 2011) where we apply a time-weakening method (Andrews, 1985) to nucleate the earthquake. The dynamic rupture process is solved using SEM2DPACK, a software package simulating wave propagation and dynamic fracture using spectral element method (Ampuero, 2009).

We apply a linear slip-weakening friction law to the fault plane:

$$\begin{cases} \mu_s - \dfrac{\mu_s - \mu_d}{D_c} D & D < D_c \\ \mu_d & D \geq D_c \end{cases} \qquad (1)$$

Where μ_s is the static friction coefficient, μ_d is the dynamic friction coefficient, D_c is the critical slip distance, and D is slip. Since the fault beneath the accretionary wedge is a bimaterial interface that can lead to instability and ill-posedness due to normal stress perturbation during rupture propagation (Cochard and Rice, 2000; Rubin and Ampuero, 2007; Ampuero and Ben-Zion, 2008), we regularize the normal stress as follows (Huang et al., 2018):

$$\frac{d\sigma^{¿}}{dt} = \frac{V^{¿}}{D_\sigma}\left(\sigma - \sigma^{¿}\right) \qquad (2)$$

Where $\sigma^{¿}$ is the effective normal stress, $V^{¿} = 1$ is the reference slip rate, and $D_\sigma = 0.2$ is the reference distance.

In light of frictional experiments on samples from the Japan Trench Fast Drilling Project (Fulton et al., 2013; Ujiie et al., 2013), we assume a low dynamic friction coefficient and shear stress near the trench. The static and dynamic friction coefficients in our models are 0.5 and 0.2, respectively. The effective normal stress linearly increases from 10 MPa at the surface to a constant value of 100 MPa below 5 km. The static (σ_s) and dynamic shear strengths (σ_d) are calculated by the product between the effective normal stress and the static and dynamic friction coefficients, respectively. The dynamic stress drop ($\Delta\sigma_d$) is the difference between the initial shear stress (τ_0) and dynamic shear strength. In our dynamic models, $\Delta\sigma_d$ is nearly equal to the static stress drop which is the difference between the initial shear stress and the final stress. Positive and negative $\Delta\sigma_d$ represents regions that promote and prohibit rupture propagation, respectively, similar to the velocity-weakening and velocity-strengthening behaviors in rate-and-state friction models. We keep a uniform critical slip distance (D_c) of 2 m at depths above 4 km and 0.25 m around the nucleation zone to facilitate rupture nucleation. We also use small deep asperities with D_c of 0.25 m to reproduce high-frequency radiation of the 2011 Tohoku-Oki earthquake in the down-dip region (Figure 2a) (Huang et al., 2012).

We determine the initial shear stress τ_0 by fitting the simulated horizontal seafloor deformation of the aw-and-sed model with the observed data. Previous studies presented various types of slip distribution for the 2011 Tohoku-Oki earthquake (Lay, 2018), but most of them revealed large shallow slip. Here we use the slip distribution constrained by the observed seafloor deformation data that includes near-trench locations (Sato et al., 2011; Kido et al., 2011; Ito et al, 2011). It should be noted that the data may have large uncertainties especially for the two points near the trench (~20 m). To reproduce the best-fitting deformation, τ_0 is 38 MPa in the nucleation zone and decreases to 18 MPa in the surrounding region. In the shallow portion of the fault, τ_0 increases to 44.6 MPa to fit the large horizontal deformation near the trench, and then linearly decreases to 1.2 MPa and remains constant till the surface (Figure 2a).

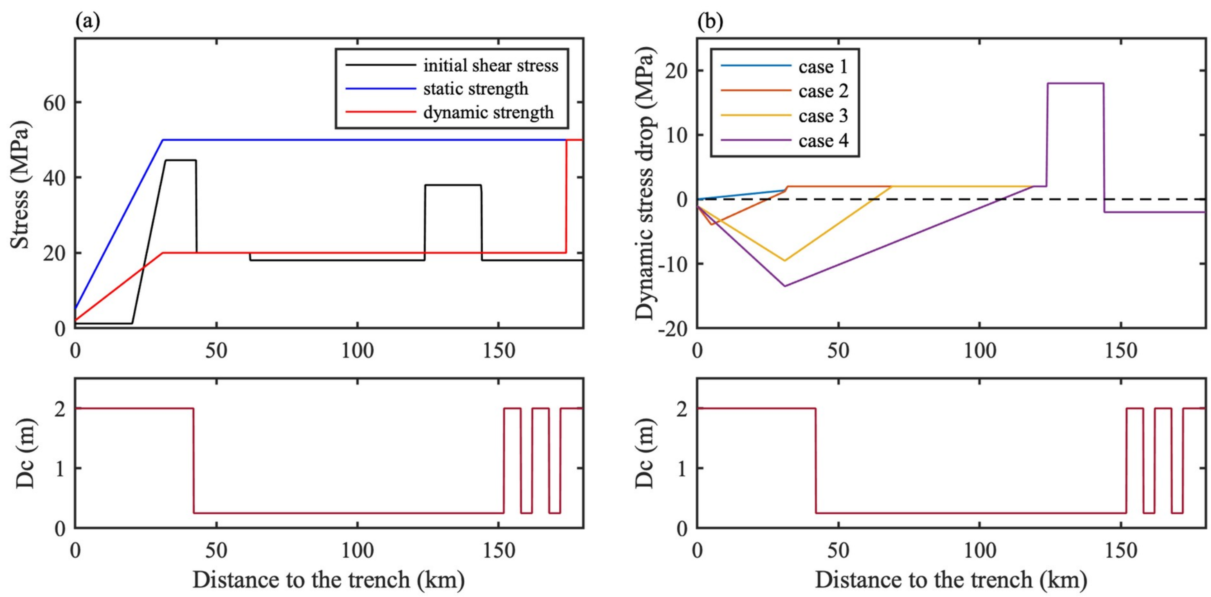

Figure 2. (a) The surface projection of the along-dip distributions of initial shear stress, static strength, dynamic strength (top), and critical slip distance (bottom) for the 2011 Tohoku-Oki earthquake. (b) The surface projection of the along-dip distributions of dynamic stress drop (top) and critical slip distance (bottom) for the four earthquake scenarios in Figure 5.

We also simulate a series of earthquake scenarios with up-dip rupture terminating at different depths. We adopt the same model geometry, fault strength, and critical slip distance as the 2011 Tohoku-Oki earthquake but change dynamic stress drop ($\Delta\sigma_d$) on the fault to constrain rupture extents. In particular, we use a shallow region of negative stress drop to prohibit rupture from reaching the trench. Figure 2b shows four earthquake cases of positive $\Delta\sigma_d$ on the entire fault (case 1), negative $\Delta\sigma_d$ at depths above 2.3 km (case 2), 7.7 km (case 3), and 16.5 km (case 4). The same as the 2011 Tohoku-Oki earthquake model, we set $\Delta\sigma_d$ at 18 MPa in the nucleation zone for the four cases.

3. Results

3.1. Slip and rupture dynamics of the 2011 Tohoku-Oki earthquake

The best-fitting aw-and-sed model of the 2011 Tohoku-Oki earthquake explains the large horizontal seafloor deformation at the two near-trench locations (Figure 3a). As the ratio between the horizontal and vertical deformation is mainly controlled by the fault-dip angle, the reproduced vertical deformation also has large values near the trench (Figure 3b). In the aw-and-sed model, the coseismic slip increases steeply from a trench-distance of 60 km to 35 km, with a peak slip reaching 83 m, similar to the maximum slip found by Iinuma et al. (2012) by inverting terrestrial GPS observations and seafloor geodetic data. Note that the aw-and-sed model results in slightly larger deformation than the observed deformation at farther distances close to the hypocentral region, due to the dynamic stress drop required for successful nucleation given the frictional parameters used in our model. With the same friction and stress conditions, however, the homogeneous model produces a much flatter slip distribution despite large dynamic stress drop on the shallow fault. Slip in the homogeneous model is lower than that in the aw-and-sed model along the fault, especially in the shallow region, with the peak slip reduced by 25% (Figure 3c). As a result, the largest horizontal and vertical seafloor deformation are reduced by 29% and 22%, respectively (Figure 3a and 3b).

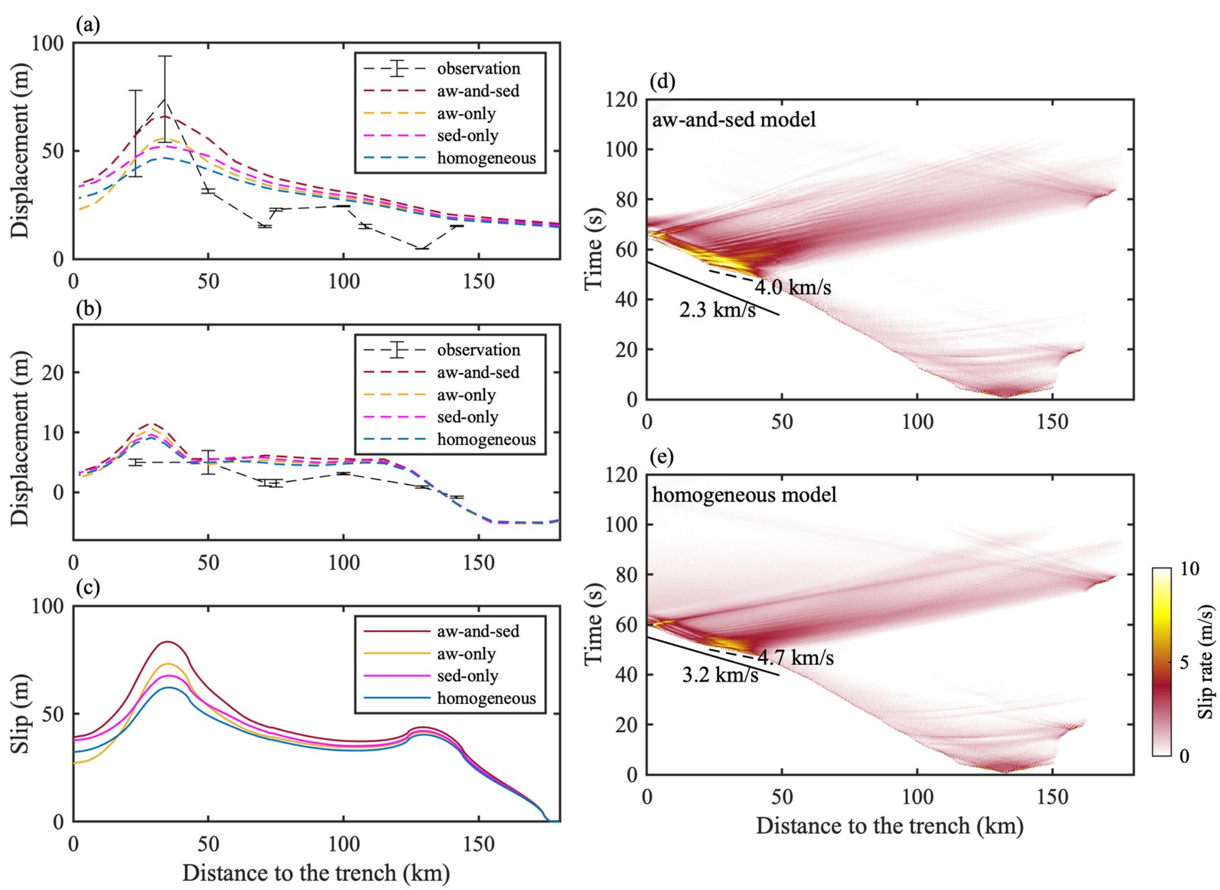

Figure 3. Surface deformation, fault slip, and slip rate during the 2011 Tohoku-Oki earthquake. (a) Horizontal surface deformation, (b) vertical surface deformation, and (c) surface projection of fault slip distributions produced by the aw-and-sed, aw-only, sed-only, homogeneous models. Spatiotemporal distributions of slip rate for (d) the aw-and-sed model and (e) the homogeneous model. Black solid lines represent shear wave speeds (2.3 km/s in the accretionary wedge and 3.2 km/s in the homogeneous medium). The black dashed lines represent rupture velocities of 4.0 km/s and 4.7 km/s in the shallow portion of the aw-and-sed model and homogeneous model, respectively.

We further investigate the respective roles of the accretionary wedge and sedimentary layer on enhancing fault slip and seafloor deformation. Both structures are found to greatly enhance the peak slip and surface deformation during the 2011 Tohoku-Oki earthquake, but the accretionary wedge has a dominant influence. The peak slip of the aw-only and sed-only models is 18% and 9% larger than that of the homogeneous model at a trench-distance of 35 km, respectively, while that of the aw-and-sed model is 34% larger at the same location (Figure 3c). The percentage of increased slip in the aw-and-sed model is also larger than the sum of the percentage of increased slip in the aw-only and sed-only models along the fault (Figure 4a). We conclude that the combined effect of the two structures on the coseismic slip of the Tohoku-Oki earthquake is larger than a linear sum of their respective effects, and the same conclusion applies to the horizontal surface deformation (Figure 4b).

We note that for the aw-only model, fault slip decreases sharply in the shallow region and is smaller than that in a homogeneous medium within a trench-distance of 17 km (Figure 3c). Lotto et al. (2017) found that when accretionary wedges are large and have velocity-strengthening friction at the basement, increasing wedge compliance reduces shallow slip. Our results suggest that the negative dynamic stress drop at the base of accretionary wedges leads to a similar effect, i.e., a more rapid decline in slip and hence a slip reduction compared to a homogeneous medium. However, the results from the sed-only and aw-and-sed models (Figure 4a) indicate that the inclusion of sedimentary layers tends to promote fault slip even when the shallow fault features negative dynamic stress drop. Figures 4c and 4d show the slip rate of the aw-and-sed, aw-only, and homogeneous models at distances of 14 km (point A) and 34 km (point B) from the trench, respectively. Rupture in the aw-only model has larger peak slip rate than in the homogeneous model but shorter rise time at shallow depths (e.g., point A), which leads to smaller slip (Figure

4c). On the other hand, rupture in the aw-and-sed model features amplified slip rate (Figures 4c and 4d) and prolonged rise time (Figure 4c) compared to the aw-only model, which together results in larger slip.

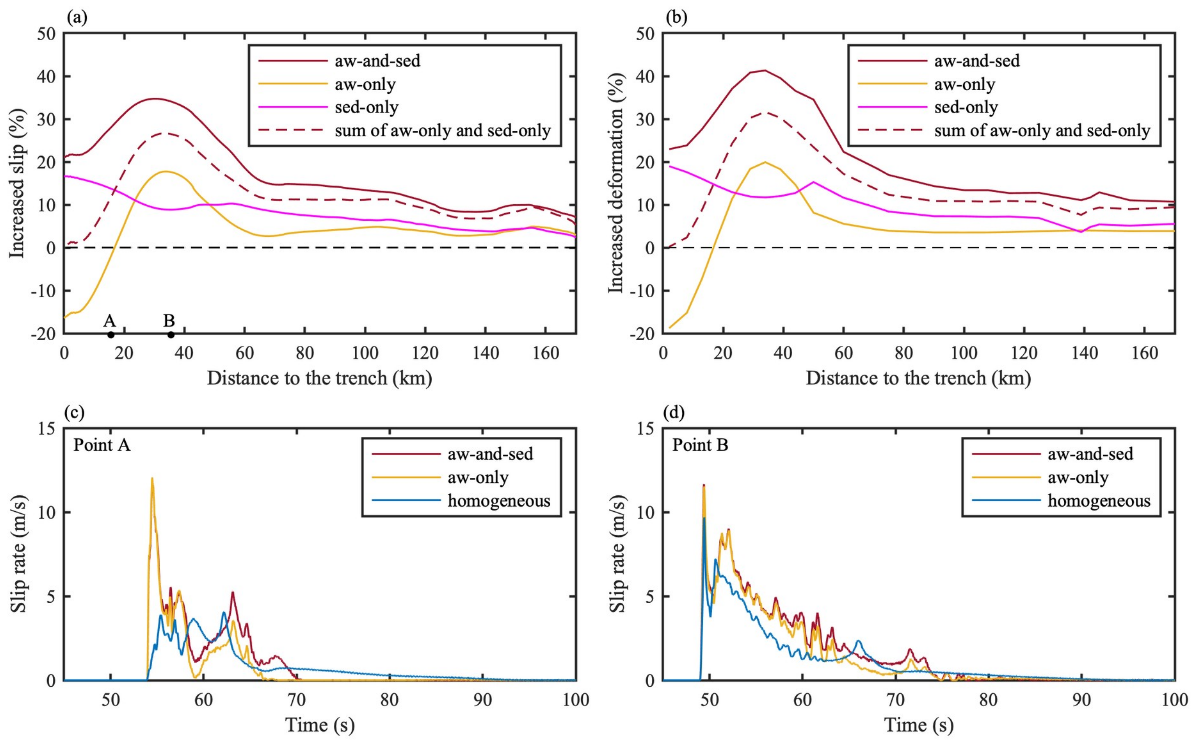

Figure 4. Percentage of increased fault slip (a) and surface horizontal deformation (b) in the non-homogeneous models compared with the homogeneous model in the 2011 Tohoku-Oki earthquake. The red dashed lines are the total percentage of the aw-only and sed-only models. (c and d) Slip rate of the aw-and-sed, aw-only, and homogeneous models at points A and B shown in (a), respectively. Note that the slip rate of the three models is regularized to the same start time.

Besides the effects on fault slip and surface deformation, the accretionary wedge also slows down shallow rupture propagation due to the lower S-wave speed in the accretionary wedge. Rupture propagates at an average speed of 2.5 km/s in the aw-and-sed model in the up-dip direction, compared to a speed of 3.4 km/s in the homogeneous medium. In both models, the shallow asperity with large dynamic stress drop causes local supershear rupture propagation (4 km/s in the aw-and-sed model and 4.7 km/s in the homogeneous model) in the up-dip direction (Figure 3d and 3e). Rupture then decelerates to subshear speeds as it propagates to the negative dynamic stress drop region.

3.2. Earthquake scenarios with different rupture extents

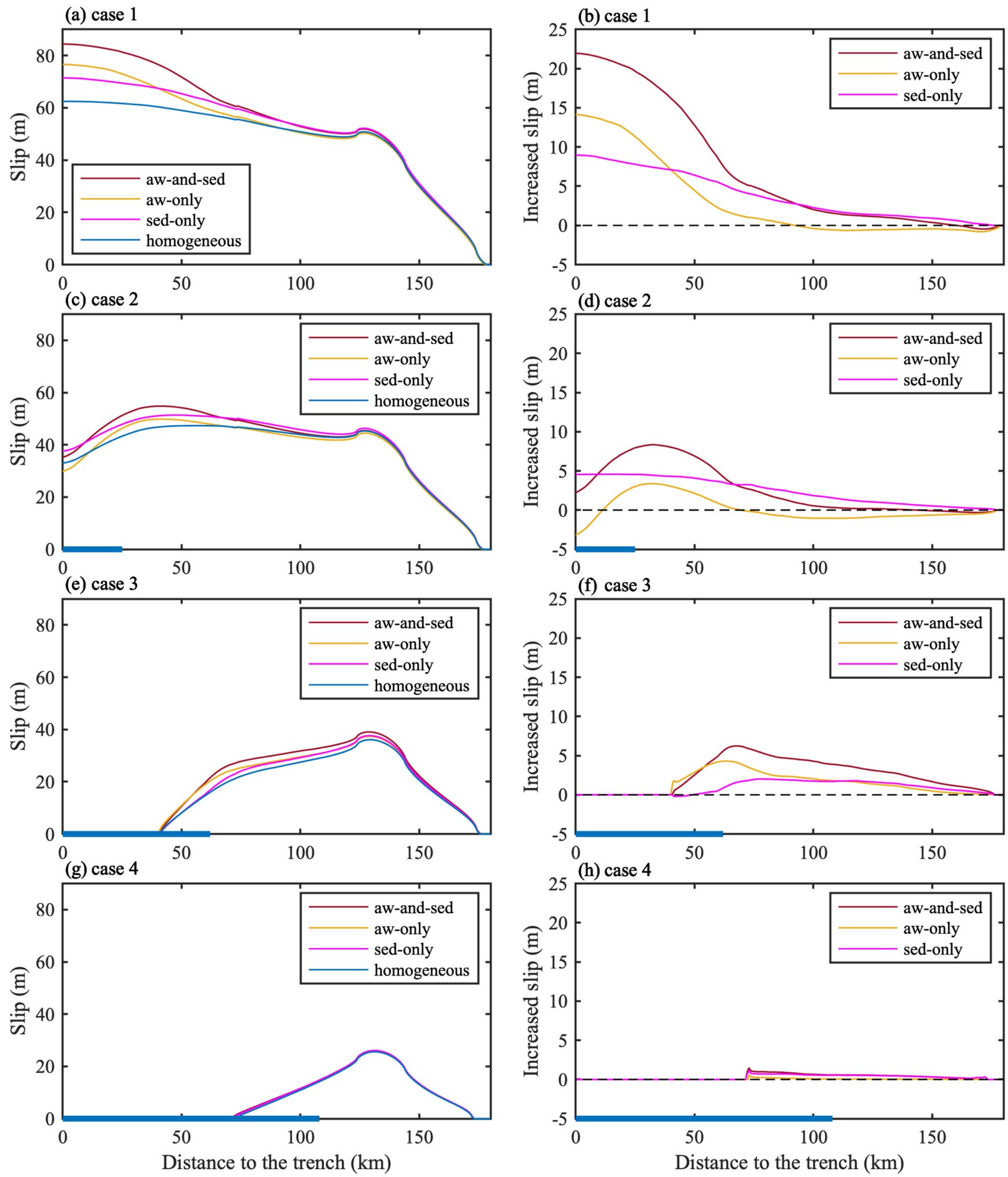

Figure 5. Fault slip and increased slip for earthquakes with rupture extents decreasing from top to bottom. The left column: comparisons of slip distribution produced by the aw-and-sed, aw-only, sed-only, and homogeneous models. The right column: increased slip of the three non-homogeneous models in

comparison to the homogeneous model. Black dashed lines indicate there is no difference between homogeneous and non-homogeneous models. Blue bold lines overlapping with the x-axis denote regions of negative dynamic stress drop.

In this section, we show that the effects of the accretionary wedge and sedimentary layer on coseismic slip and surface deformation strongly depend on the extent of the shallow rupture, which translates into earthquake magnitude given the same hypocenter location. Figure 5 shows the comparisons of coseismic slip produced by aw-and-sed, aw-only, sed-only, and homogeneous models in four earthquake scenarios when the negative $\Delta\sigma_d$ region extends from surface to depth. The negative $\Delta\sigma_d$ region acts as a barrier prohibiting rupture propagation and thus controls shallow rupture extents. When $\Delta\sigma_d$ is positive on the entire fault, which leads to rupture through the trench, both the accretionary wedge and sedimentary layer greatly enhance fault slip (Figures 5a and 5b). In the case of negative $\Delta\sigma_d$ beneath the outer wedge, rupture reaches the trench but fault slip declines near the trench (Figures 5c and 5d). The accretionary wedge and sedimentary layer greatly enhance the peak slip, but the accretionary wedge leads to a sharper decline in near-trench slip, causing smaller slip than that in the homogeneous model. However, the aw-and-sed model has larger slip on the shallow fault due to the sedimentary layer, which supports the previous finding that the inclusion of sedimentary layers promotes fault slip. As rupture terminates before reaching the trench due to the larger negative $\Delta\sigma_d$ region, the enhancement effects of the accretionary wedge and sedimentary layer on fault slip diminish (Figures 5e and 5f). For the case when rupture does not reach the bottom of the accretionary wedge, the sedimentary layer slightly enhances fault slip and the accretionary wedge has almost no influence (Figures 5g and 5h).

In conclusion, a sedimentary layer always has a positive effect on the coseismic slip in the four earthquake scenarios, while an accretionary wedge may cause smaller near-trench slip when the dynamic stress drop is negative on the shallow fault. However, a combination of the two structures tends to enhance coseismic slip. The combined effect is significant when rupture reaches the trench and diminishes as the up-dip rupture terminates at deeper depth.

3.3. Effects of the accretionary wedge and sedimentary layer on ground accelerations

We find that the co-existence of the accretionary wedge and sedimentary layer prolongs ground acceleration durations and amplifies peak ground accelerations, but the combined effect behaves differently depending on the shallow rupture extents of earthquakes. In the case of the 2011 Tohoku-Oki earthquake, the ground acceleration durations in the aw-and-sed model are significantly prolonged as shown in the accelerograms recorded at two stations inside and outside the accretionary wedge (Figure 6a). Guo et al. (2016) and Kaneko et al. (2019) suggested that accretionary wedges can lead to longer durations of long-period ground motions, due to the surface waves generated from the seaward edge of accretionary wedges or the reverberations of seismic waves within accretionary wedges. To quantify the ground acceleration amplification, the amplification factor is defined as a ratio of peak ground accelerations between non-homogeneous and homogeneous models. We calculate the average amplification factors in two frequency ranges: 0.1-0.5 Hz, 0.5-2.0 Hz. We find that for all stations on the overriding plate, the ground accelerations of the aw-and-sed model are significantly amplified at both 0.1-0.5 Hz and 0.5-2.0 Hz (Figure 6b). The maximum amplification effects for both frequency ranges happen in the vicinity of the accretionary wedge. Inside the accretionary wedge, the amplification effect on the ground acceleration at 0.5-2.0 Hz is larger than at 0.1-0.5 Hz (Figure 6b).

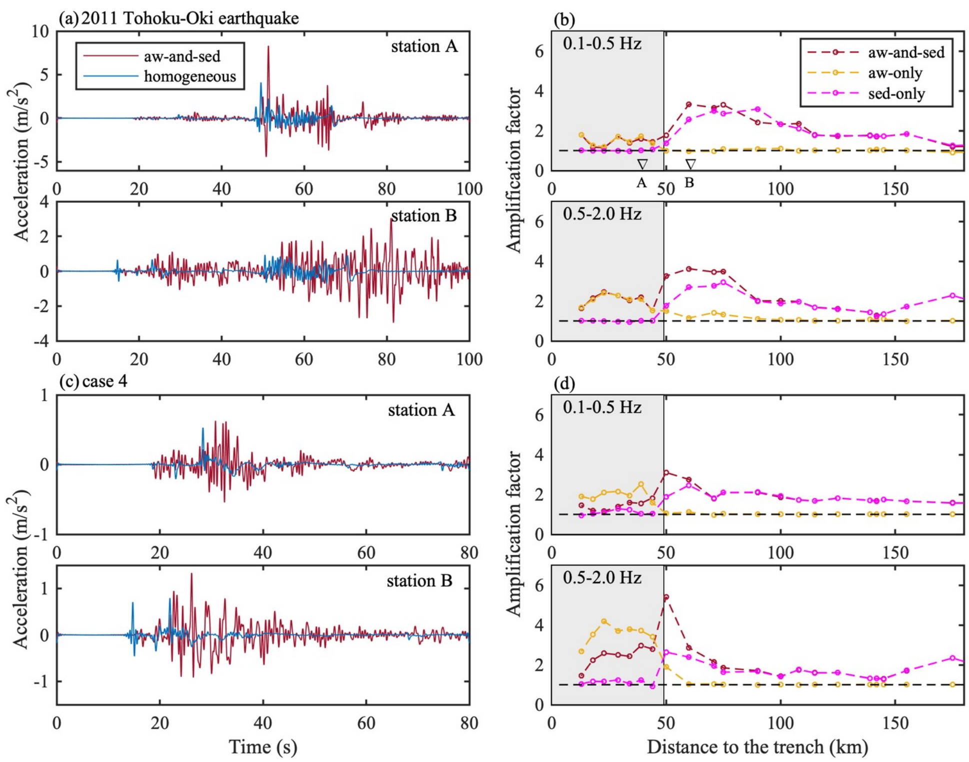

Figure 6. (a) Comparisons of horizontal accelerograms between the aw-and-sed and homogeneous models; (b) Averaged amplification factors for horizontal ground accelerations at 0.1-0.5 Hz and 0.5-2.0 Hz produced by the three non-homogeneous models during the 2011 Tohoku-Oki earthquake. The shaded zone is the region inside the accretionary wedge. Black dashed lines represent a value of 1. A and B are stations located inside and outside the accretionary wedge, respectively. (c) and (d) have the same representation as (a) and (b), respectively, but for the smaller earthquake in Figure 5g.

When rupture does not reach the bottom of the accretionary wedge (case 4 in Figures 5g and 5h), the two structures can greatly enhance ground accelerations, though they have a minimal influence on fault slip. However, the combined effect on the ground acceleration amplification is not always larger than the respective effects. Similar to the 2011 Tohoku-Oki earthquake, the aw-and-sed model produces longer durations at stations inside and outside the accretionary wedge (Figure 6c). In the aw-and-sed model, the maximum amplification effects on the ground accelerations at 0.1-0.5 Hz and 0.5-2.0 Hz are located at the landward edge of the accretionary wedge where the combined effect of the accretionary wedge and the sedimentary layer is significantly greater than their linear sum (Figure 6d bottom). Similar to the 2011 Tohoku-Oki earthquake, the amplification effect inside the accretionary wedge exhibits distinct frequency-dependence with ground accelerations at 0.5-2.0 Hz in the aw-and-sed and aw-only models being more amplified than those at 0.1-0.5 Hz (Figure 6d). These results suggest that dynamic wave interaction inside an accretionary wedge can cause more ground acceleration amplification at high frequencies. The frequency-dependent effect was also observed in the 2016 southeast off-Mie earthquake. Kubo et al. (2019) found that the offshore acceleration response spectra at periods of 0.5-8 s largely exceeds values obtained from the empirical attenuation relationship while that at shorter periods of 0.12 and 0.25 s follows the empirical relationship. The results were interpreted as a large site amplification effect due to an accretionary wedge.

We notice that for all the stations inside the accretionary wedge, the amplification factors of the aw-and-sed model are obviously smaller than those of the aw-only model, with the ground accelerations at 0.5-2.0 Hz being greatly suppressed in particular (Figure 6d bottom). Thus, for earthquake rupture that does not reach the accretionary wedge, the existence of a sedimentary layer may weaken the amplification effect of the accretionary wedge on ground accelerations inside the accretionary wedge, which may be attributed to wave interference between the two structures.

4. Discussion

4.1. Implications for stress drop estimation of the 2011 Tohoku-Oki earthquake

Stress release and accumulation on faults are essential to assess regional earthquake hazards. As an important parameter in controlling the source mechanism, stress drop during the 2011 Tohoku-Oki earthquake has been investigated by different methods. These studies consider a homogeneous medium, a 1-D layered medium without sedimentary layers, or a 1-D layered medium with sedimentary layers. Brown et al. (2015) estimated a mean stress drop of 2.3 ± 1.3 MPa and a peak value of 40 MPa from 40 rupture models of the 2011 Tohoku-Oki earthquake assuming a uniform rigidity of 40 GPa. Assuming a 1-D model without sediment structures, Xie and Cai (2018) constrained an average stress drop of 6.3 MPa from stress inversion of the observed coseismic deformation. Koketsu et al. (2011) calculated an average stress drop of 4.8 MPa from the source model constructed through joint inversion of teleseismic, strong motion, and geodetic datasets with sedimentary layers considered in velocity structure.

Here our best-fitting aw-and-sed model reveals a maximum stress drop of 25 MPa on the shallow asperity in the 2011 Tohoku-Oki earthquake (Figure S1). However, to reproduce the same observed peak deformation near the trench, the maximum stress drop on the shallow asperity is ~27 MPa, 27MPa, and 30 MPa for the aw-only, sed-only, and homogeneous models, respectively (Figure S1). This indicates that stress drop on the shallow fault evaluated from fault slip or surface deformation can be overestimated by 20% when accretionary wedge and sedimentary layer are not considered, as the co-existence of the two structures greatly enhances the coseismic slip during the 2011 Tohoku-Oki earthquake. We also calculate the average stress drop from different models using integrated stress drop divided by the rupture length. The average stress drop in the aw-and-sed, aw-only, sed-only, and homogeneous models is 2.5 MPa, 2.7 MPa, 2.8 MPa, and 3.2MPa, respectively. The average stress drop in the homogeneous model is 28% larger than that in the aw-and-sed model. Our results suggest that for other large megathrust earthquakes that reach the accretionary wedge, both average and maximum stress drop estimated for a homogeneous medium may be overestimated.

4.2. Implications for global megathrust earthquakes

In the last century, besides the northern Japan trench, M_w 8.5 and above earthquakes also occurred in the Aleutians, Alaska, Kuril, Kamchatka, south-central Chile, and Sumatra subduction zones. These subduction zones all feature a co-existence of accretionary wedges and sedimentary layers. The two structures could be important factors in controlling large subduction zone earthquakes. Wells et al. (2003) illustrated that rupture zones of great subduction zone earthquakes tend to underlie the forearc basins. Most seaward part of an accretionary wedge exhibits a velocity-strengthening behavior, which is generally thought to impede up-dip rupture (Wang & Hu, 2006). Ma and Nie (2019) showed that coseismic yielding of plentiful sediments in the northern Japan trench margin can induce large inelastic uplift and diminish slip near the trench. However, Gulick et al. (2011) suggested that accreted sediments near the Sunda trench were dewatered and compacted, which allowed a velocity-weakening behavior and hence facilitated the rupture of the 2004 M_w 9.2 Sumatra-Andaman earthquake to the trench. Lotto et al.

(2017) pointed out that more compliant accretionary wedges in most cases cause greater shallow fault slip, but larger accretionary wedges with velocity-strengthening friction reduce slip.

Our results indicate that accretionary wedges and sedimentary layers greatly enhance coseismic slip for earthquakes that propagate to trenches or terminate at shallow depths, allowing subduction zones to have a greater potential to accommodate large earthquakes. In the 2004 M_w 9.2 Sumatra-Andaman earthquake, the coseismic rupture occurred largely beneath the accretionary wedge in the southern part of the rupture area (Gulick et al., 2011). The upper bound of the coseismic slip during the 2010 M_w 8.8 Chile earthquake reached the toe of the accretionary wedge with peak slips near the trench (Yue et al., 2014). The up-dip limit of the 1960 M_w 9.5 great Chile earthquake extends further seaward (Contreras−Reyes et al., 2010). The accretionary wedges and sedimentary layers may have played important roles in enhancing the shallow slip during these large earthquakes. Besides, a co-existence of accretionary wedges and sedimentary layers significantly prolongs and amplifies ground motions near the accretionary wedge (Figure 6), which may induce submarine landslide failure. In Cascadia where great earthquakes are the most likely to occur in the Pacific Northwest United States, ground motion intensity in a future megathrust earthquake was predicted based on kinematic rupture models that do not account for the dynamic effects of low-velocity near-fault structures (Wirth et al., 2018). With wide accretionary wedges and sedimentary layers covering the continental plate (Gulick et al., 1998; Parsons et al., 1998), our results suggest that evaluations of Cascadia seismic hazards should consider the possibility of longer and larger ground motions produced by the two structures as well.

4.3. Limitations and future works

Since our focus is to evaluate the influence of accretionary wedges and sedimentary layers on the along-dip rupture process, 2-D models that do not account for along-strike variations are used in this work. In the rupture zone of the 2011 Tohoku-Oki earthquake, the wedge-shaped sediments appear in the northern area of the epicenter with dimensions varying along the Japan trench, but in the southern area, the sediments extend in the down-dip direction as a channel-like unit (Tsuru et al., 2002). Future numerical models should be directed towards 3-D rupture simulations to address the influence of along-strike heterogeneity on rupture features. On the other hand, we analyze the effects of the accretionary wedge and sedimentary layer on coseismic slip and ground motions assuming purely elastic properties. However, the nature of an accretionary wedge or a sedimentary layer can have viscoelastic and plastic behaviors, which may diminish slip and reduce surface deformation (Ma & Nie, 2019). Since the effect of sedimentary structures should be a combination of elastic and inelastic effects, whether it promotes fault slip also depends on which behavior is in a dominant role. A more realistic approximation of accretionary wedges and sedimentary layers in future works is to incorporate viscoelasticity and plasticity.

5. Conclusions

Our dynamic rupture simulations of the 2011 Tohoku-Oki earthquake show that the co-existence of the accretionary wedge and sedimentary layer significantly enhances coseismic slip in the shallow region and greatly amplifies ground accelerations near the accretionary wedge. When the shallow fault features negative stress drop, an accretionary may cause smaller near-trench slip, while a combination with a sedimentary layer tends to enhance fault slip. The enhancement effects of the two structures are pronounced when rupture reaches the trench and diminish as the up-dip rupture is deeper. When earthquake rupture does not reach accretionary wedges, a sedimentary layer has a slight enhancement effect on the coseismic slip while an accretionary wedge has almost no influence. But a co-existence of the two structures can greatly amplify ground accelerations on the overriding plate. We suggest that for large megathrust earthquakes that reach shallow fault, stress drop estimated from coseismic slip or surface deformation can be overestimated when accretionary wedges and sedimentary layers are neglected. Our 2-D dynamic rupture models provide a fundamental understanding of how the low-velocity near-fault structures can impact subduction zone earthquake processes and highlight the importance of considering the effects of accretionary wedges and sedimentary layers in seismic observations and numerical modeling of subduction zone earthquakes.

Data Availability Statement

We used Trelis (https://coreform.com/products/trelisnew/) to mesh the geometrical model. The numerical simulations were solved using SEM2DPACK version 2.3.8 (http://www.sourceforge.net/projects/sem2d/), and simulation results were visualized by Matlab. The input files to reproduce simulation results and the scripts to plot figures in this paper are available on UM Deep Blue (https://doi.org/10.7302/rerb-bd58).

Acknowledgments

X. Li acknowledges the support from China Scholarship Council (NO.201904910712). Y. Huang acknowledges the funding support from the National Science Foundation (Grant Award EAR-1663769). We thank Prithvi Thakur and Marlon D. Ramos for the helpful suggestions to improve this paper. X. Li also thanks Marlon D. Ramos for helping with the procedures of SEM2DPACK and Trelis.

References

Ampuero, J. P. (2009). SEM2DPACK: A spectral element method tool for 2D wave propagation and earthquake source dynamics, User's Guide, version 2.3.6. Retrieved from http://www.sourceforge.net/projects/sem2d/

Ampuero, J.-P., & Ben-Zion, Y. (2008). Cracks, pulses and macroscopic asymmetry of dynamic rupture on a biomaterial interface with velocity- weakening friction. *Geophysical Journal International,* 173(2), 674–692. https://doi.org/10.1111/j.1365-246X.2008.03736.x

Andrews, D. J. (1985). Dynamic plane−strain shear rupture with a slip−weakening friction law calculated by a boundary integral method. *Bulletin of the Seismological Society of America,* 75(1), 1-21.

Brocher, T. M., Fuis, G. S., Fisher, M. A., Plafker, G., Moses, M. J., Taber, J. J., & Christensen, N. I. (1994). Mapping the megathrust beneath the northern Gulf of Alaska using wide-angle seismic data. *Journal of Geophysical Research,* 99(B6), 11663-11685. https://doi.org/10.1029/94JB00111

Brown, L., Wang, K., & Sun, T. (2015). Static stress drop in the Mw 9 Tohoku−oki earthquake: Heterogeneous distribution and low average value. *Geophysical Research Letters,* 42, 10595-10600. https://doi.org/10.1002/2015GL066361

Chu, R., Wei, S., Helmberger, D. V., Zhan, Z., Zhu, L., &Kanamori, H. (2011). Initiation of the great Mw 9.0 Tohoku-Oki earthquake. *Earth and Planetary Science Letters,* 308, 277-283. https://doi.org/10.1016/j.epsl.2011.06.031

Cochard, A., & Rice, J. R. (2000). Fault rupture between dissimilar materials: Ill-posedness, regularization, and slip-pulse response. *Journal of Geophysical Research,* 105(B11), 25,891–25,907. https://doi.org/10.1029/2000JB900230

Contreras−Reyes, E., Flueh, E. R., & Grevemeyer, I. (2010). Tectonic control on sediment accretion and subduction off south central Chile: Implications for coseismic rupture processes of the 1960 and 2010 megathrust earthquakes. *Tectonics,* 29, TC6018. https://doi.org/10.1029/2010TC002734

Cubas, N., Lapusta, N., Avouac, J.-P., & Perfettini, H. (2015). Numerical modeling of long-term earthquake sequences on the NE Japan megathrust: Comparison with observations and implications for fault friction. *Earth and Planetary Science Letters,* 419, 187-198. https://doi.org/10.1016/j.epsl.2015.03.002

Divins, D. (2003). *Total Sediment Thickness of the World's Oceans & Marginal Seas.* Boulder, CO: NOAA National Geophysical Data Center.

Duan, B. (2012). Dynamic rupture of the 2011 Mw 9.0 Tohoku-Oki earthquake: Roles of a possible subducting seamount. *Journal of Geophysical Research,* 117, B05311. https://doi.org/10.1029/2011JB009124

Flueh, E. R., Vidal N., Ranero, C. R., Hojka, A., von Huene, R., Bialas, J., et al. (1998). Seismic investigation of the continental margin off− and onshore Valparaiso, Chile. *Tectonophysics,* 288, 251–263.

Fujiwara, T., Kodaira, S., No, T., Kaiho, Y., Takahashi, N., & Kaneda, Y. (2011). The 2011 Tohoku-Oki earthquake: Displacement reaching the trench axis. *Science,* 334, 1240. https://doi.org/10.1126/science.1211554

Fulton, P., Brodsky, E., Kano, Y., Mori, J., Chester, F., Ishikawa, T., et al. (2013). Low coseismic friction on the Tohoku-Oki fault determined from temperature measurements. *Science,* 342, 1214-1217. https://doi.org/10.1126/science.1243641

Gulick, S. P. S., Austin, J. A., McNeill, L. C., Bangs, N. L. B., Martin, K. M., Henstock, T. J., et al. (2011). Updip rupture of the 2004 Sumatra earthquake extended by thick indurated sediments. *Nature Geoscience,* 4, 453-456. https://doi.org/10.1038/ngeo1176

Gulick, S. P. S., Meltzer, A. M., & Clarke, S. H. (1998). Seismic structure of the southern Cascadia subduction zone and accretionary prism north of the Mendocino triple junction. *Journal of Geophysical Research,* 103(B11), 27207-27222. https://doi.org/10.1029/98JB02526

Guo, Y., Koketsu, K., & Miyake, H. (2016). Propagation mechanism of long-period ground motions for offshore earthquakes along the Nankai trough: Effects of the accretionary wedge. *Bulletin of the Seismological Society of America,* 106(3), 1176-1197. https://doi.org/10.1785/0120150315

Holbrook, W. S., Lizarralde, D., McGeary, S., Bangs, N., & Diebold, J. (1999). Structure and composition of the Aleutian island arc and implications for continental crustal growth. *Geology,* 27(1), 31-34. https://doi.org/10.1130/0091-7613(1999)027<0031:SACOTA>2.3.CO;2

Huang, Y. (2018). Earthquake rupture in fault zones with along−strike material heterogeneity. *Journal of Geophysical Research: Solid Earth,* 123, 9884-9898. https://doi.org/10.1029/2018JB016354

Huang, Y., Ampuero, J.-P., & Kanamori, H. (2014). Slip-weakening models of the 2011 Tohoku-Oki earthquake and constraints on stress drop and fracture energy. *Pure and Applied Geophysics,* 171, 2555-2568. https://doi.org/10.1007/s00024-013-0718-2

Huang, Y., Meng, L., & Ampuero, J.-P. (2012). A dynamic model of the frequency-dependent rupture process of the 2011 Tohoku-Oki earthquake. *Earth, Planets and Space,* 64, 1061-1066. https://doi.org/10.5047/eps.2012.05.011

Iinuma, T., Hino, R., Kido, M., Inazu, D., Osada, Y., Ito, Y., et al. (2012). Coseismic slip distribution of the 2011 off the Pacific Coast of Tohoku Earthquake (M9.0) refined by means of seafloor geodetic data. *Journal of Geophysical Research,* 117, B07409. https://doi.org/10.1029/2012JB009186

Ito, Y., Tsuji, T., Osada, Y., Kido, M., Inazu, D., Hayashi, Y., et al. (2011). Frontal wedge deformation near the source region of the 2011 Tohoku-Oki earthquake. *Geophysical Research Letters,* 38, L00G05. https://doi.org/10.1029/2011GL048355

Kaneko, Y., Ito, Y., Chow, B., Wallace, L. M., Tape, C., Grapenthin, R., et al. (2019). Ultralong duration of seismic ground motion arising from a thick, low−velocity sedimentary wedge. *Journal of Geophysical Research: Solid Earth,* 124, 10347-10359. https://doi.org/10.1029/2019JB017795

Kato, N., & Yoshida, S. (2011). A shallow strong patch model for the 2011 great Tohoku−oki earthquake: A numerical simulation. *Geophysical Research Letters,* 38, L00G04. https://doi.org/10.1029/2011GL048565

Kido, M., Osada, Y., Fujimoto, H., Hino, R., & Ito, Y. (2011). Trench-normal variation in observed seafloor displacements associated with the 2011 Tohoku-Oki earthquake. *Geophysical Research Letters,* 38, L24303. https://doi.org/10.1029/2011GL050057

Kimura, G., Hina, S., Hamada, Y., Kameda, J., Tsuji, T., Kinoshita, M., & Yamaguchi, A. (2012). Runaway slip to the trench due to rupture of highly pressurized megathrust beneath the middle trench slope: The tsunamigenesis of the 2011 Tohoku earthquake off the east coast of northern Japan. *Earth and Planetary Science Letters,* 339-340, 32-45. https://doi.org/10.1016/j.epsl.2012.04.002

Klaeschen, D., Belykh, I., Gnibidenko, H., Patrikeyev, S., & von Huene, R. (1994). Structure of the Kuril Trench from seismic reflection records. *Journal of Geophysical Research,* 99(B12), 24173-24188. https://doi.org/10.1029/94JB01186

Kodaira, S., Iwasaki, T., Urabe, T., Kanazawa, T., Egloff, F., Makris, J., & Shimamura, H. (1996). Crustal structure across the middle Ryukyu trench obtained from ocean bottom seismographic data. *Tectonophysics,* 263, 39-60. https://doi.org/10.1016/S0040-1951(96)00025-X

Koketsu, K., Yokota, Y., Nishimura, N., Yagi, Y., Miyazaki, S., Satake, K., et al. (2011). A unified source model for the 2011 Tohoku earthquake. *Earth and Planetary Science Letters,* 310, 480-487. https://doi.org/10.1016/j.epsl.2011.09.009

Kopp, C., Fruehn, J., Flueh, E. R., Reichert, C., Kukowski, N., Bialas, J., & Klaeschen, D. (2000). Structure of the makran subduction zone from wide-angle and reflection seismic data. *Tectonophysics,* 329, 171-191. https://doi.org/10.1016/S0040-1951(00)00195-5

Kopp, H., Flueh, E. R., Klaeschen, D., Bialas, J., & Reichert, C. (2001). Crustal structure of the Central Sunda margin at the onset of oblique subduction. *Geophysical Journal International,* 147, 449-474. https://doi.org/10.1046/j.0956-540X.2001.01547.x

Kozdon, J. E., & Dunham, E. M. (2013). Rupture to the Trench: Dynamic rupture simulations of the 11 March 2011 Tohoku earthquake. *Bulletin of the Seismological Society of America,* 103(2B), 1275-1289. https://doi.org/10.1785/0120120136

Krabbenhöft, A., Bialas, J., Kopp, H., Kukowski, N., & Hübscher, C. (2004). Crustal structure of the Peruvian continental margin from wide-angle seismic studies. *Geophysical Journal International,* 159, 749-764. https://doi.org/10.1111/j.1365-246X.2004.02425.x

Kubo, H., Nakamura, T., Suzuki, W., Dhakal, Y. P., Kimura, T., Kunugi, T., et al. (2019). Ground-motion characteristics and nonlinear soil response observed by donet1 seafloor observation network during the 2016 southeast off-Mie, Japan, Earthquake. *Bulletin of the Seismological Society of America,* 109(3), 976-986. https://doi.org/10.1785/0120170296

Lay, T. (2018). A review of the rupture characteristics of the 2011 Tohoku-oki Mw 9.1 earthquake. *Tectonophysics,* 733, 4-36. https://doi.org/10.1016/j.tecto.2017.09.022

Lotto, G. C., Dunham, E. M., Jeppson, T. N., & Tobin, H. J. (2017). The effect of compliant prisms on subduction zone earthquakes and tsunamis. *Earth and Planetary Science Letters,* 458, 213-222. https://doi.org/10.1016/j.epsl.2016.10.050

Ma, S., & Hirakawa, E. T. (2013). Dynamic wedge failure reveals anomalous energy radiation of shallow subduction earthquakes. *Earth and Planetary Science Letters,* 375, 113-122. https://doi.org/10.1016/j.epsl.2013.05.016

Ma, S., & Nie, S. (2019). Dynamic Wedge Failure and Along-Arc Variations of Tsunamigenesis in the Japan Trench Margin. *Geophysical Research Letters,* 46, 8782-8790. https://doi.org/10.1029/2019GL083148

Mitsui, Y., Kato, N., Fukahata, Y., & Hirahara, K. (2012). Megaquake cycle at the Tohoku subduction zone with thermal fluid pressurization near the surface. *Earth and Planetary Science Letters,* 325-326, 21-26. https://doi.org/10.1016/j.epsl.2012.01.026

Murphy, S., Di Toro, G., Romano, F., Scala, A., Lorito, S., Spagnuolo, E., et al. (2018). Tsunamigenic earthquake simulations using experimentally derived friction laws. *Earth and Planetary Science Letters,* 486, 155–165. https://doi.org/10.1016/j.epsl.2018.01.011

Nakanishi, A., Shiobara, H., Hino, R., Kodaira, S., Kanazawa, T., & Shimamura, H. (1998). Detailed subduction structure across the eastern Nankai Trough obtained from ocean bottom seismographic profiles. *Journal of Geophysical Research,* 103(B11), 27151-27168. https://doi.org/10.1029/98JB02344

Noda, H., & Lapusta, N. (2013). Stable creeping fault segments can become destructive as a result of dynamic weakening. *Nature,* 493, 518-521. https://doi.org/10.1038/nature11703

Parsons, T., Trehu, A. M., Luetgert, J. H., Miller, K., Kilbride, F., Wells, R. E., et al. (1998). A new view into the Cascadia subduction zone and volcanic arc: Implications for earthquake hazards along the Washington margin. *Geology,* 26(3), 199-202. https://doi.org/10.1130/0091-7613(1998)026<0199:ANVITC>2.3.CO;2

Rubin, A. M., & Ampuero, J.-P. (2007). Aftershock asymmetry on a biomaterial interface. *Journal of Geophysical Research,* 112, B05307. https://doi.org/10.1029/2006JB004337

Sallarès, V., Dañobeitia, J. J., & Flueh, E. R. (2001). Lithospheric structure of the Costa Rican Isthmus: Effects of subduction zone magmatism on an oceanic plateau. *Journal of Geophysical Research,* 106(B1), 621-643. https://doi.org/10.1029/2000JB900245

Sato, M., Ishikawa, T., Ujihara, N., Yoshida, S., Fujita, M., Mochizuki, M., & Asada, A. (2011). Displacement above the hypocenter of the 2011 Tohoku-Oki earthquake. *Science,* 332, 1395. https://doi.org/10.1126/science.1207401

Tsuru, T., Park, J.-O., Miura, S., Kodaira, S., Kido, Y., & Hayashi, T. (2002). Along-arc structural variation of the plate boundary at the Japan Trench margin: Implication of interplate coupling. *Journal of Geophysical Research,* 107(B12), 2357. https://doi.org/10.1029/2001jb001664

Ujiie, K., Tanaka, H., Saito, T., Tsutsumi, A., Mori, J., & Toczko, S. (2013). Low coseismic shear stress on the Tohoku-Oki megathrust determined from laboratory experiments. *Science,* 342, 1211-1214. DOI: 10.1126/science.1243485

van Zelst, I., Wollherr, S., Gabriel, A.−A., Madden, E. H., & van Dinther, Y. (2019). Modeling megathrust earthquakes across scales: one−way coupling from geodynamics and seismic cycles to dynamic rupture. *Journal of Geophysical Research: Solid Earth,* 124, 11414–11446. https://doi.org/10.1029/ 2019JB017539

von Huene, R., Klaeschen, D., Gutscher, M., & Fruehn, J. (1998). Mass and fluid flux during accretion at the Alaskan margin. *The Geological Society of America Bulletin,* 110(4), 468-482. https://doi.org/10.1130/0016-7606(1998)110<0468:MAFFDA>2.3.CO;2

Wang, K., & Hu, Y. (2006). Accretionary prisms in subduction earthquake cycles: The theory of dynamic Coulomb wedge. *Journal of Geophysical Research,* 111, B06410. https://doi.org/10.1029/2005JB004094

Wells, R. E., Blakely, R. J., Sugiyama, Y., Scholl, D. W., & Dinterman, P. A. (2003). Basin−centered asperities in great subduction zone earthquakes: A link between slip, subsidence, and subduction erosion? *Journal of Geophysical Research,* 108, 2507. https://doi.org/10.1029/2002JB002072

Wirth, E., Frankel, A., Marafi, N., Vidale, J., & Stephenson, W. (2018). Broadband synthetic seismograms for magnitude 9 earthquakes on the Cascadia megathrust based on 3D simulations and stochastic synthetics, Part 2: Rupture parameters and variability. Bulletin of the Seismological Society of America, 108(5A), 2370– 2388. https://doi.org/10.1785/0120180029

Xie, Z., & Cai, Y. (2018). Inverse method for static stress drop and application to the 2011 Mw9.0 Tohoku-Oki earthquake. *Journal of Geophysical Research: Solid Earth,* 123, 2871-2884. https://doi.org/10.1002/2017JB014871

Yue, H., Lay, T., Rivera, L., An, C., Vigny, C., Tong, X., & Báez Soto, J. C. (2014). Localized fault slip to the trench in the 2010 Maule, Chile Mw = 8.8 earthquake from joint inversion of high−rate GPS, teleseismic body waves, InSAR, campaign GPS, and tsunami observations. *Journal of Geophysical Research: Solid Earth,* 119, 7786-7804. https://doi.org/10.1002/2014JB011340

AGU PUBLICATIONS

Journal of Geophysical Research: Solid Earth

Supporting Information for

The enhancement of coseismic slip and ground motion due to the accretionary wedge and sedimentary layer in the 2011 Tohoku-Oki earthquake

Xian Li[1 2], Yihe Huang[3]

[1]Key Laboratory of Earth and Planetary Physics, Institute of Geology and Geophysics, Chinese Academy of Sciences, Beijing 100029, China.

[2]College of Earth and Planetary Sciences, University of Chinese Academy of Sciences, Beijing 100049, China.

[3]Department of Earth and Environmental Sciences, University of Michigan, Ann Arbor, MI 48109, USA.

Corresponding author: Xian Li (lixian@mail.iggcas.ac.cn)

Contents of this file

Introduction

The Supporting Information includes a figure which shows best-fitting horizontal seafloor deformation reproduced by the aw-and-sed, aw-only, sed-only, and homogeneous models and the stress drop distribution.

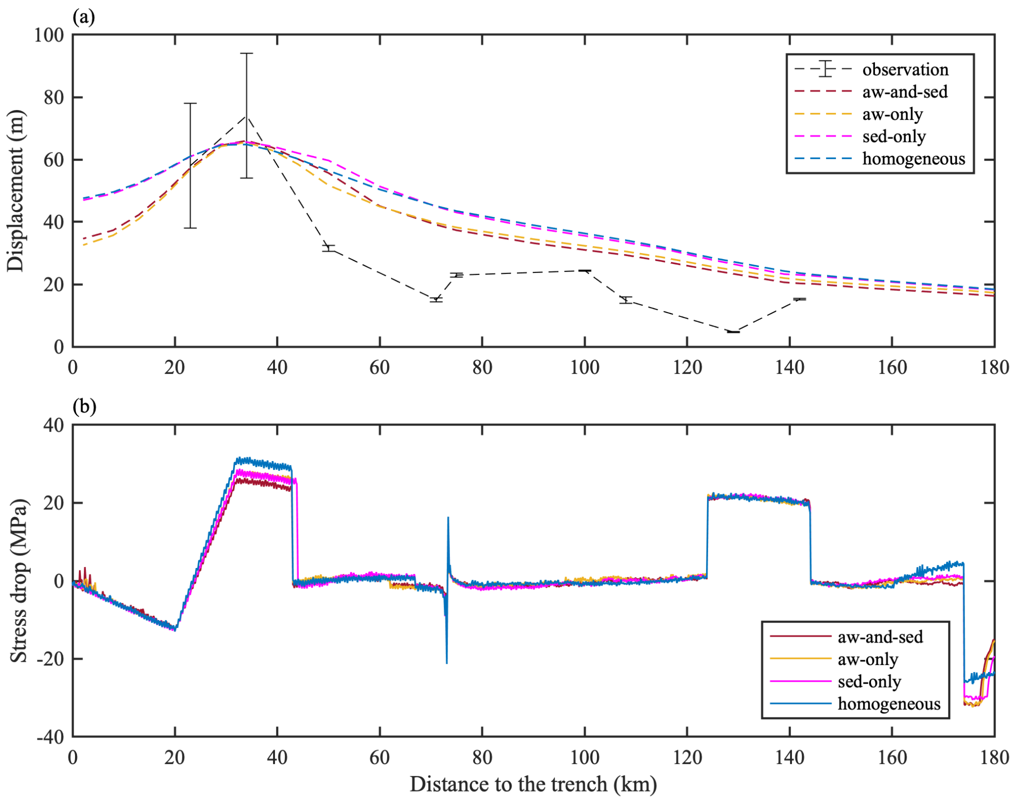

Figure S1. (a) Best-fitting horizontal seafloor deformation reproduced by the aw-and-sed, aw-only, sed-only, and homogeneous models in comparison with the observed deformation. (b) Static stress drop of the four models.